UNIVERSITY OF SOUTH BOHEMIA IN ČESKÉ BUDĚJOVICE
FACULTY OF SCIENCE

STRUCTURAL BIOLOGY APPROACH TO BIOTECHNOLOGICAL PROBLEMS

PhD THESIS

Iuliia Iermak, MSc

Supervisor: Doc. Ivana Kuta Smatanova, PhD
University of South Bohemia Ceske Budejovice
Faculty of Science - Institute of Chemistry and Biochemistry
& Center for Nanobiology and Structural Biology
Institute of Microbiology ASCR

České Budějovice 2017

This thesis should be cited as:

Iermak, I. 2017: Structural biology approach to biotechnological problems. PhD Thesis Series, No 6, University of South Bohemia, Faculty of Science, České Budějovice, Czech Republic, 133 pp.

ANNOTATION

Enhancement of the catalytic performance of various enzymes in the reaction systems requires advanced studies of enzymes' structure-function relationships. The obtained information is used to engineer favourable enzyme variants exhibiting beneficial properties for applications in biotechnology. In the thesis X-ray crystallographic analysis was successfully employed for the structure-functional characterization of the glyceraldehyde dehydrogenase from thermophilic bacterium *Thermoplasma acidophilum* (*Ta*AlDH). This enzyme is one of the key enzymes in the cell-free system for the production of ethanol or isobutanol from glucose. The second part of the thesis describes optimization by structure-guided engineering of the haloalkane dehalogenase LinB from the soil bacterium *Sphingobium japonicum* UT26, used for the effective degradation of halogenated environmental pollutants.

Declaration [in Czech]

Prohlašuji, že svoji disertační práci jsem vypracoval samostatně pouze s použitím pramenů a literatury uvedených v seznamu citované literatury.

Prohlašuji, že v souladu s § 47b zákona č. 111/1998 Sb. v platném znění souhlasím se zveřejněním své disertační práce, a to v úpravě vzniklé vypuštěním vyznačených částí archivovaných Přírodovědeckou fakultou elektronickou cestou ve veřejně přístupné části databáze STAG provozované Jihočeskou univerzitou v Českých Budějovicích na jejích internetových stránkách, a to se zachováním mého autorského práva k odevzdanému textu této kvalifikační práce. Souhlasím dále s tím, aby toutéž elektronickou cestou byly v souladu s uvedeným ustanovením zákona č. 111/1998 Sb. zveřejněny posudky školitele a oponentů práce i záznam o průběhu a výsledku obhajoby kvalifikační práce. Rovněž souhlasím s porovnáním textu mé kvalifikační práce s databází kvalifikačních prací Theses.cz provozovanou Národním registrem vysokoškolských kvalifikačních prací a systémem na odhalování plagiátů.

České Budějovice .....

Iuliia Iermak

This thesis originated from a partnership of the Faculty of Science, University of South Bohemia, and the Center for Nanobiology and Structural Biology, Institute of Microbiology of the Czech Academy of Sciences, supporting doctoral studies in the Biophysics study program.

Financial support
Czech Science Foundation grants GAČR 207/12/0775 and GAČR 17-24321S; The Czech Academy of Sciences and Deutscher Akademischer Austauschdienst bilateral mobility project DAAD-15-09.

The thesis is based on the following publications:

I. Iermak I, Degtjarik O, Steffler F, Sieber V, Kuta Smatanova I (2015) Crystallization behaviour of glyceraldehyde dehydrogenase from Thermoplasma acidophilum. Acta Cryst F 71:1475-1480. (IF = 0.647)

Iuliia Iermak devised experimental strategies, performed crystallization and X-ray data collection experiments, analyzed data and wrote the manuscript (jointly with Ivana Kuta Smatanova).

II. Iermak I, Mesters JR, Steffler F, Sieber V, Kuta Smatanova I (2017) Structural features of glyceraldehyde dehydrogenase from *Thermoplasma acidophilum*. *Manuscript*

Iuliia Iermak conceived the idea (jointly with IKS), performed structure solution, refinement, deposition and analysis, and wrote the manuscript (jointly with IKS and JRM).

III. Brezovsky J, Babkova P, Degtjarik O, Fortova A, Gora A, Iermak I, Rezacova P, Dvorak P, Kuta Smatanova I, Prokop Z, Chaloupkova R, Damborsky J (2016) Engineering a *de novo* transport tunnel. ACS Catalysis, 6(11):7597-7610. (IF = 9.307)

Iullia Iermak helped with crystallization experiments, data collection, structure refinement and deposition for one of LinB variants.

IV. Iermak I, Mesters JR, Chaloupkova R, Damborsky J, Kuta Smatanova I (2017) Structural features of haloalkane dehalogenase LinB variants. *Manuscript*.

Iuliia Iermak conceived the idea (jointly with IKS), designed experimental strategies, conducted experiments, analyzed the data and wrote the manuscript (jointly with IKS and JRM).

Prohlašuji, že se Iuliia Iermak podílela na společných publikacích v uvedeném rozsahu.

Doc. Ivana Kuta Smatanova, PhD

ACKNOWLEDGEMENTS

I would like to thank everybody who helped and supported me during the very important period in my life – my PhD study.

First of all, I want to thank my supervisor, Ivana Kuta Smatanova, for continuous support and advice in difficult moments, as well as encouragement of almost all my ideas. Thanks to her outstanding scientific and organizational skills we always had friendly and motivating atmosphere in our group.

I want to specifically acknowledge my scientific advisor Jeroen Mesters for constant willingness to help and for introducing me to the world of X-ray crystallography. His great ideas enormously facilitated my scientific research and always helped me to look at problems at a different angle.

My deepest gratitude belongs to my colleagues: Radka Chaloupkova, Jiri Damborsky, Volker Sieber and Fabian Steffler for providing me with protein samples and cooperation; Oksana Degtjarik for helping with my first steps in protein crystallization; Tatyana Prudnikova for useful tips and tricks in crystallization and crystallography; Magda Vojtova for constant assistance in the lab; and Pavel Grinkevich for his help with data collections and sharing his knowledge in molecular biology.

My special thanks belong to my summer school students Alzbeta Roeselova, Mykyta Markevych, David Novak, Bianka Kohegyi, Sara Comduhr and Antje Schoelzel for helping me at different stages of my projects and for bringing fresh ideas.

I would like to thank administration and technical staff of CNSB and PrF for providing all necessary facilities to make my study and research easy and comfortable.

I want to thank all my friends from Nove Hrady and Ceske Budejovice: Alex Bondar, Kate Sviridova, Saurabh Pandey, Anna Gurina, Daria Malakhova, Deepika Kale and Jost Ludwig who made my life and work pleasant and productive.

Finally, I cannot overstate my gratitude to my sister Eva and my husband Dima as well as to my parents for understanding and support of all my efforts, great patience and helping to make so many good decisions in my life.

Dedicated to my family

TABLE OF CONTENTS

LIST OF ABBREVIATIONS

CECF - crude extract cell-free systems
SEP - synthetic enzymatic pathway
GDH - glucose dehydrogenase
DHAD - gluconate/glycerate/dihydroxyacid dehydratase
KDGA - 2-keto-3-desoxygluconate aldolase
AlDH - aldehyde dehydrogenase
*Ta*AlDH - glyceraldehyde dehydrogenase from *Thermoplasma acidophilum*
PDC - pyruvate decarboxylase
ADH - alcohol dehydrogenase
ALS - acetolactate synthase
KARI - ketolacid reductoisomerase
KDC - 2-ketoacid decarboxylase
EDB - ethylene dibromide
γ-HCCH - γ-hexachlorocyclohexane
DCE - 1,2-dichloroethane

1. INTRODUCTION

1.1. Prologue and aims of the research

Scrutiny of various features, developed by different organisms for the adaptation to their environmental conditions, has always been a source of new ideas for scientists and engineers in their work. For instance, in 1903, brothers Wright have successfully created the first heavier-than-air aircraft, inspired by pigeons' flight. Nowadays, biologically inspired engineering employs biological principles for new applications in industry, medicine and environment protection. Not only the natural principles are employed but also biological systems themselves. For thousands of years living organisms were modified for biotechnological applications in food industry, agriculture and medicine; e.g. using specific yeasts in brewing or production of antibiotic penicillin from the fungi *Penicillium*.

Using biotechnological methods for the production of various chemicals is of particular importance as it is more environmentally gentle approach compared to a fossil-resources-based approach. A number of cell-based as well as cell-free techniques have been developed for synthesis of various compounds, starting from small organic molecules to proteins. The second component of environment protection is the limitation of waste emissions into the atmosphere and ground water, and the decay of existing pollutants. Presently, numerous methods are being developed for the biodegradation of environmental pollutants. Microorganisms with modified metabolic pathways or individual enzymes with engineered substrate specificity are used for such purposes.

In terms of bio-catalysis, cell-free processes are generally more effective because *ex-vivo* enzyme reaction mixtures can tolerate higher concentrations of substrates and products as compared to the equivalent cell-based approaches. Another advantage of cell-free systems is that the supplied substrates do not get involved in cell's metabolism, resulting in non-desired side-product formation. Enhancement of the catalytic performance of the applied enzymes in the *ex-vivo* reaction systems requires advanced studies of enzymes' structure-function relationships. The obtained information is used to engineer favourable enzyme variants exhibiting beneficial properties for application in cell-free biotechnological processes.

This thesis comprises two projects. The first one is focused on the structure-functional characterization of the glyceraldehyde dehydrogenase from thermophilic bacterium *Thermoplasma acidophilum* (*Ta*AlDH), which is one of the key enzymes in the cell-free system for the production of ethanol or isobutanol from glucose. The second part of this work concerns optimization by structure-guided engineering of the haloalkane dehalogenase LinB from the soil bacterium *Sphingobium japonicum* UT26, used for the effective degradation of halogenated environmental pollutants.

1.2. Bioproduction of chemicals

The outcome of the dependence on fossil fuels in the production of various chemicals is the eventual depletion of natural fossil resources. During the past few decades, the focus has considerably shifted from using natural fossil fuels to using organisms or even synthetic bioprocesses for the production of industrially relevant compounds. For this, biological systems are modified and/or parts of different natural systems are assembled to produce non-natural products (1). Several techniques for microbial bioproduction and for cell-free biosynthesis have been successfully implemented for interesting target molecules such as ethanol (2), butanol (3, 4), hydrogen (5), precursors for pharmaceuticals (6), amino acids (7), vitamins (8) and even plastics (9).

Although bioproduction of chemicals, fuels and other materials require further improvement, in particular, enhancing product tolerance, increasing product yields and creating commercially relevant large-scale production systems, feasibility and utility of such approaches was demonstrated (10).

1.2.1. Cell-free biosynthesis

The first established biotechnological processes for the synthesis of organic chemicals were cell-based systems, e.g. bacterial cells and yeast. They are predominantly used for production of different kinds of organic solvents (biofuels), as well as for a wide variety of other chemicals used in pharmacy and industry.

However, the primary drawback of the microbial fermentation process is that the major fraction of energy from the supplied nutrients is utilized by the cells for proliferation and maintaining their integrity rather than to produce the desired product (11). Moreover, the involvement of substrates into cell

metabolism and non-desired by-product formation may lower both stoichiometric conversion rates and product yields, and even low concentrations of products can significantly affect microbial cell viability and productivity (3, 12). The functioning of microbial systems is also restricted to physiological ambient conditions (neutral pH, mild temperature), while running reactions at elevated temperatures would conveniently increase reaction rates (13).

The abovementioned limitations can be addressed through the development of synthetic cell-free enzyme systems by reprogramming the existing and designing novel metabolic pathways (14, 15). Several factors need to be considered for the construction of such systems: cofactor balance, thermodynamics, reaction equilibrium, and product separation and purification (16).

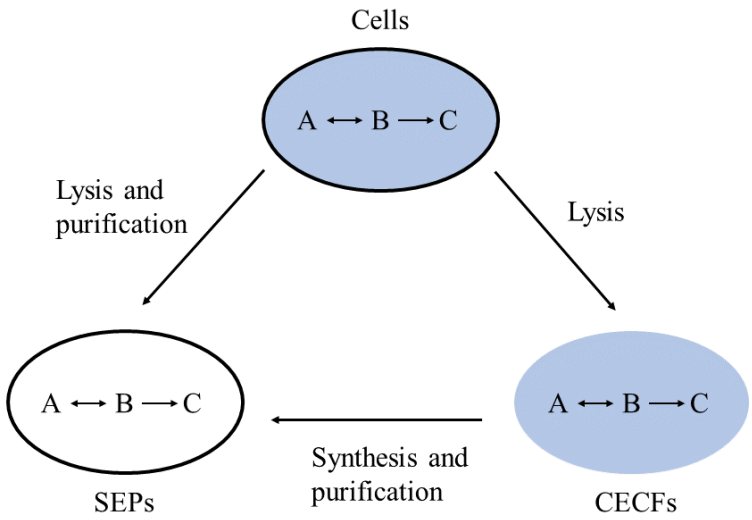

Figure 1.1. The relations between synthesis platforms in synthetic biology: microbial fermentation, crude extract cell-free systems (CECFs) and synthetic enzymatic pathways (SEPs) (14).

Cell-free approaches can be divided into two big groups: crude extract cell-free systems (CECFs) and synthetic enzymatic pathways (SEPs) (14, 17) (Fig. 1.1). The first example of a cell-free system was shown by Eduard Buchner in 1897: yeast extract effectiveness was demonstrated for the conversion of sugar to ethanol and carbon dioxide (18) for which Buchner got awarded the

Nobel Prize in Chemistry in 1907. Currently cell-free approaches have practical applications in cellular metabolic pathways investigation, protein and peptide synthesis and evolution, small molecule production, and non-natural product synthesis (14).

A major advantage of SEPs is their flexibility in rational programming of biosynthetic networks. For instance, a SEP for hydrogen synthesis is composed of thirteen proteins from different organisms, including rabbit, spinach, *Pyrococcus furiosus*, *Saccharomyces cerevisiae*, and *Escherichia coli*. Construction of this SEP allowed for high yields of 12 H_2 molecules per glucose compared to only 4 H_2 molecules per glucose obtained with anaerobic fermentation (5).

Major challenges for cell-free synthetic biology include integration and activation of efficient and predictable enzyme networks at low cost and large scale by bridging *in vitro* and *in vivo* functionality. Nevertheless, cell-free systems have the potential to change the approach to study, control, and modify cellular ensembles for biomanufacturing of any chemical from renewable resources.

1.2.2. Cell-free enzyme cascade for biosynthesis of alcohols

Usage of biofuels is already widespread in industry, especially of ethanol. However, butanol possesses a higher energy density, lower vapor pressure, and lower hygroscopicity than ethanol, therefore showing advantages in terms of commercial use, storage and transportation (3). Apart from being used as a biofuel, ethanol and butanol are utilized as intermediates in chemical synthesis, as solvents for a wide variety of chemicals and in textile industry applications.

Recently, a completely artificial minimized reaction cascade was constructed for the conversion of glucose to ethanol or isobutanol (Fig. 1.2). The conversion of glucose to pyruvate, the central intermediate in this cascade, is achieved by modified non-phosphorylative Entner-Doudoroff-Pathway derived from hyperthermophilic archaea (19). Only four enzymes are needed: glucose dehydrogenase (GDH), gluconate/glycerate/dihydroxyacid dehydratase (DHAD), 2-keto-3-desoxygluconate aldolase (KDGA), and glyceraldehyde dehydrogenase (AlDH). 2-keto-3-desoxygluconate is split into pyruvate and glyceraldehyde, which is then relayed for pyruvate production as well. In the subsequent two-step reaction, pyruvate can be converted to acetaldehyde and

acetaldehyde to ethanol by the action of pyruvate decarboxylase (PDC) and alcohol dehydrogenase (ADH). Alternatively, pyruvate can be used for isobutanol production. Two pyruvate molecules are joined by acetolactate synthase (ALS) to produce acetolactate, which is further converted by ketolacid reductoisomerase (KARI) to dihydroxyisovalerate. DHAD then catalyzes the conversion of dihydroxyisovalerate into 2-ketoisovalerate. The enzymes 2-ketoacid decarboxylase (KDC) and an ADH are used to obtain isobutanol via isobutyraldehyde.

This artificial pathway is completely redox balanced and requires only a single molecular shuttle NAD^+, which is recycled in the reaction cascade. All enzymes for the cascade were selected according to their degree of substrate specificity, stability under reaction conditions and overall activity (20). One of the advantages of this artificial cascade is that the enzymes were found to remain highly active in up to 4% (v/v) isobutanol, a condition where bacterial cells are no more capable to survive or maintain an active metabolism (3).

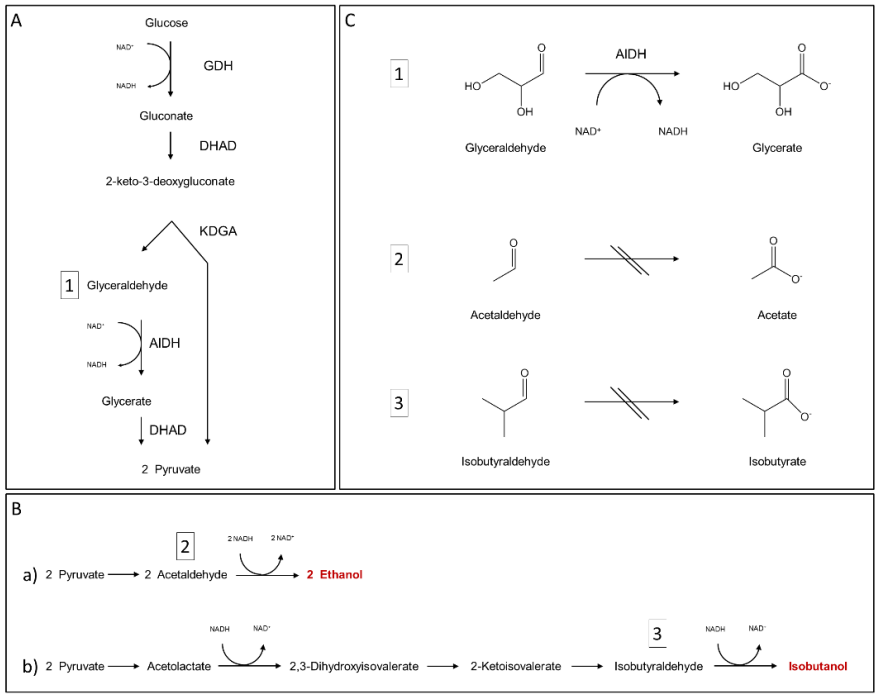

Figure 1.2. Schematic representation of the cell-free enzyme cascade for biosynthesis of ethanol and isobutanol. In the first part of the reaction (A) glucose is converted into two molecules of pyruvate; (B) requirements for AlDH functioning within the cascade: high specificity towards glyceraldehyde and no acceptance of acetaldehyde or isobutyraldehyde; (C) conversion of pyruvate to ethanol or isobutanol (adopted from 21).

In this system, molar yield of 57.4 % in 19 h for ethanol and 53% in 23 h for isobutanol were achieved, demonstrating the successful recycling of NAD^+ and NADH, as well as successful redirection of glyceraldehyde resulting from 2-keto-3-desoxygluconate cleavage towards pyruvate (20).

1.2.3. Glyceraldehyde dehydrogenase from *Thermoplasma acidophilum* and its implementation in the synthetic cascade for biosynthesis of ethanol and isobutanol

Glyceraldehyde dehydrogenase from *Thermoplasma acidophilum* (*Ta*AlDH) belongs to the aldehyde dehydrogenase superfamily and is involved in the downstream portion of the non-phosphorylated Entner–Doudoroff pathway. This pathway is used by thermoacidophilic archaea such as *Thermoplasma acidophilum* and *Sulfolobus solfataricus* to metabolize D-glucose (22).

One of the key reactions for the conversion of glyceraldehyde to pyruvate in the artificial enzyme cascade, described above, is the oxidation of D-glyceraldehyde to D-glycerate. The corresponding enzyme, aldehyde dehydrogenase (AlDH), should ideally combine the following properties: high thermostability and tolerance towards the solvent, high activity, acceptance of NAD^+ as a cofactor and high substrate specificity (21). $NADP^+$-dependent *Ta*AlDH was found to meet the requirement of high specificity for glyceraldehyde as it does not accept other aldehydes such as acetaldehyde or isobutyraldehyde, which are downstream reaction intermediates. Although it was successfully purified and implemented in the cascade (20, 23), protein engineering is needed to improve the enzyme's acceptance for NAD^+ as this cofactor is used as the only electron carrier in the cascade. *Ta*AlDH was found to function at isobutanol concentration of up to 9%. Although such concentration of the solvent is already higher than the microbial tolerance limit, it is desirable to increase the enzyme stability toward isobutanol and ethanol, preferably up to the concentration where phase separation occurs (about 12%).

Optimized variants of *Ta*AlDH were obtained by the directed evolution approach (21). *Ta*AlDH F34M+S405N variant showed an overall 8.5-fold increase in volumetric activity, a slight increase in NAD^+ acceptance and a 9-fold improvement of the catalytic efficiency with NAD^+ compared to wild type

(K_m = 17.6 mM, k_{cat} = 10.99 s^{-1}). *Ta*AlDH F34M+Y399C+S405N displays a 55.7-fold increase in activity of the wildtype enzyme and showed improved NAD^+ acceptance and a slight improvement in solvent tolerance (K_m = 116.7 mM, k_{cat} = 10.54 s^{-1}). Further optimization of *Ta*AlDH requires an understanding of the structural basis for enzyme functioning.

1.3. Bioremediation of polluted environment

A wide variety of chemical compounds used at some point in different industries, technologies and in agriculture are poorly biodegradable. Such chemicals accumulate and persist in the soil and ground water even decades after their use has been forbidden. Depending on the chemical nature these compounds can have various negative impacts on climate, biodiversity in polluted regions and human health. Therefore, diverse methods have already been developed or are currently being designed for the degradation of environmental pollutants, including biodegradation by bacteria or purified enzymes as well as abiotic techniques.

1.3.1. Halogenated environmental pollutants and biotechnological approach to remediation

Halogenated compounds, e.g. 1,2-dibromoethane (ethylene dibromide, EDB), γ-hexachlorocyclohexane (γ-HCCH), 1,2-dichloroethane (DCE), etc., represent one of the largest groups of environmental pollutants. 1,2-Dibromoethane was historically used as a pesticide and soil fumigant in various crops, as well as a scavenger in lead-containing automobile and aircraft fuels to prevent build-up of lead oxide deposits (24, 25). γ-HCCH has been used as an agricultural pesticide and as treatment for pediculosis (26), whereas DCE is utilized in industry, as an intermediate for the production of certain chemicals, and as an organic solvent (24). A number of halogenated compounds exhibit neurotoxic and carcinogenic effects, and were banned from use under the Stockholm Convention on persistent organic pollutants (27). Despite the ban, halogenated compounds pollution remains a significant issue due to the long half-life of such chemicals, the large amounts used in agriculture in the past, and leakages from the storage tanks (24, 28, 29). Thus, methods for the detection and remediation of polluted environments are needed. The use of microorganisms for bioremediation is especially attractive because of economic

and environmental reasons.

Various studies have shown possibilities for abiotic transformation of halogenated alkanes by iron sulfide (30) or hydrogen sulfide (31), and for biodegradation under anaerobic conditions by methanogenic bacteria and *Dehalococcoides sp.* (32, 33) as well as aerobic biodegradation (34, 35) and cometabolism by different bacteria (36, 37). It was also shown that stimulation by addition of ethane, propane or phenol to indigenous bacteria in presence of inorganic nutrients increases the microbial activity in degradation of EDB (38, 39). It is advantageous to use biostimulation of native microorganisms, well-suited to the environment, for bioremediation.

Analysis of the bacteria participating in aerobic mineralization of halogenated compounds revealed that enzymes of the haloalkane dehalogenases family (EC 3.8.1.5) are responsible for one of the key reactions in the pathway. They catalyze the cleavage of the carbon-halogen bond in halogenated aliphatic pollutants, resulting in formation of a corresponding alcohol, a halide ion and a proton (40). Apart from applications in bioremediation (41, 42), haloalkane dehalogenases can be potentially utilized in biosensing of pollution (43, 44), biosynthesis (45), cellular imaging and protein immobilization (46). Furthermore, haloalkane dehalogenases have become an important model system for the *in-silico* study of molecular principles of enzymatic catalysis (47, 48).

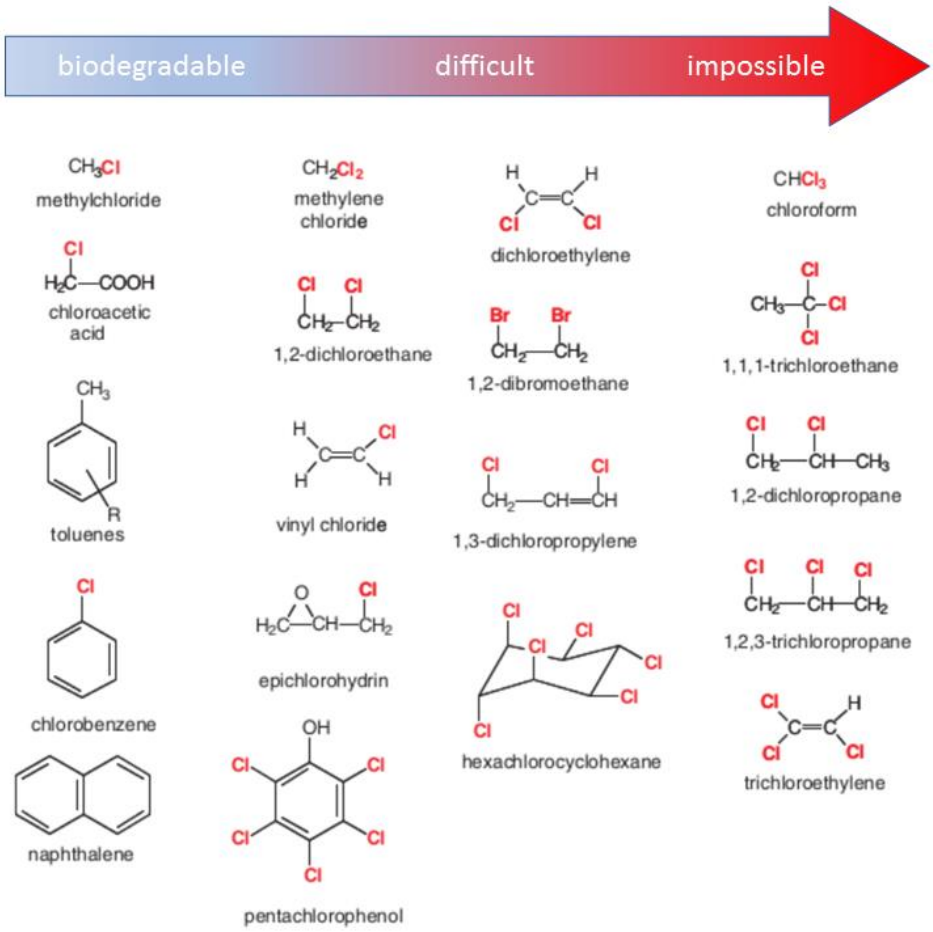

Figure 1.3. Degradability of some aliphatic and aromatic compounds: from readily biodegradable substrates on the left to recalcitrant compounds on the right. The compounds in the middle are biodegradable, but organisms are not ubiquitous and success depends strongly on environmental conditions (adopted from 40).

Due to a scarcity of enzymes that catalyze crucial steps in catabolism of halogenated compounds, these xenobiotic chemicals display resistance to biodegradation, low-molecular weight ones in particular (40). As these synthetic chemicals are somewhat water soluble and bioavailable, investigation and engineering of haloalkane dehalogenases substrate specificity could improve their conversion by bacterial metabolic pathways.

1.3.2. Structure and reaction mechanism of haloalkane dehalogenases

A number of haloalkane dehalogenase structures have already been determined, such as DhlA from *Xanthobacter autotrophicus* GJ10 (49), LinB

from *Sphingobium japonicum* UT26 (50), DbeA from *Bradyrhizobium elkanii* USDA94 (51), DhaA from *Rhodococcus rhodochrous* NCIMB 13064 (52), etc. Structurally, haloalkane dehalogenases belong to α/β-hydrolase structural superfamily (53) and consist of two domains: an α/β-hydrolase core domain and a helical cap domain, which lies on top of the core domain (Fig. 1.4). The active site is located in a hydrophobic cavity at the interface between the two domains and is connected to the protein surface by several tunnels.

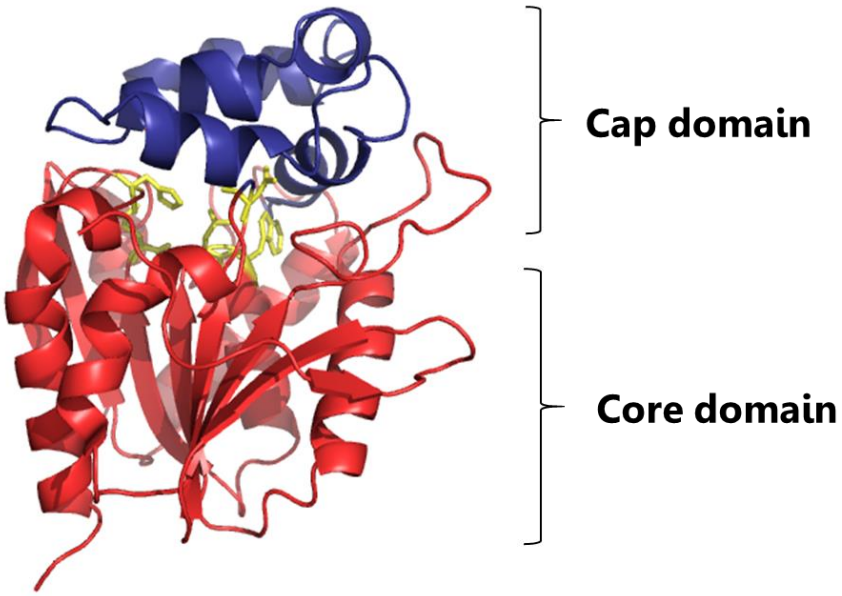

Figure 1.4. Cartoon representation of wild-type LinB structure: cap domain is shown in blue, core domain is shown in red and active site residues are yellow (PDB ID 1CV2, 50).

The active sites of dehalogenases contain a catalytic triad of three amino acids that participate in dehalogenation reaction; a nucleophilic aspartate, a basic histidine and a catalytic aspartic or glutamic acid (54). The majority of haloalkane dehalogenases with known structures contain a halide anion binding site as part of the active site. Halide-binding site consists of two highly conserved amino acids, tryptophan-tryptophan (55) or tryptophan-asparagine (51, 52). These two amino acid side chains stabilize the halogen atom of the substrate and then the halide anion formed during the dehalogenation reaction.

The catalytic mechanism of the haloalkane dehalogenase reaction includes four main steps: (i) substrate binding in the active site; (ii) nucleophilic

attack of the aspartate on the substrate, resulting in formation of an alkyl-enzyme intermediate and a halide ion; (iii) nucleophilic addition of a water molecule to the intermediate; (iv) release of the reaction products (55).

The composition of catalytic residues, architecture and solvation of the active-site cavity, the geometry and dynamics of the access tunnels, that connect the buried active site with the surrounding solvent, define substrate specificity and affect the catalytic efficiency of haloalkane dehalogenases (56). Therefore, optimization of haloalkane dehalogenases for biotechnological applications includes engineering of the active-site cavity as well as the access tunnels (45, 57, 58).

1.3.3. Optimization of haloalkane dehalogenase LinB from *Sphingobium japonicum* UT26 for use in bioremediation

Haloalkane dehalogenase LinB from the soil bacterium *Sphingobium japonicum* (formerly, *Sphingomonas paucimobilis*) UT26 has a broad substrate specificity and therefore a high potential for application in bioremediation of halogen-compound-polluted environments (59). Substrates for LinB are monochloroalkanes (C3 to C10), dichloroalkanes, bromoalkanes and chlorinated aliphatic alcohols (60).

LinB is the second enzyme in a pathway of biodegratation of γ-hexachlorocyclohexane, and effectively debrominates 1,2-dibromoethane to bromoethanol. The active site of LinB is considerably larger in comparison to the other dehalogenases; it has high binding affinity for larger substrates, with optimal chain length of six carbon atoms (61).

Different LinB variants were constructed for studying the effect of mutations on the enzyme's functionality and to enhance its catalytic properties (57). The main steps of dehalogenation reaction mechanism of the wild-type LinB have been visualized using molecular dynamics simulations (62). Several variants of the enzyme were crystallized and diffraction data were collected (63, 64), as well as enzyme activity assays and measurements of product release rates were carried out (57, 65, 66) in order to compare the behavior of wild-type LinB with the variant proteins. Further analysis of LinB variant crystal structures combined with activity essays will need to follow in order to complete the picture of haloalkane dehalogenase LinB functioning and application in bioremediation.

1.4. X-ray crystallography as a tool for protein structure determination

X-ray crystallography along with cryo-electron microscopy and nuclear magnetic resonance spectroscopy is one of the principal methods for the determination of atomic or close-to-atomic details of macromolecule structures. Biomolecules of any size are suitable for X-ray diffraction analysis, starting from small globular soluble proteins (e. g. lysozyme) up to huge protein-protein or protein-RNA complexes, such as the photosystem or the ribosome.

To reveal atomic details of a protein structure, an imaging technique must use electromagnetic radiation with a wavelength comparable to or shorter than the diameter of the electron cloud of an atom (~ 1 Å). This makes X-rays, with its wavelength range of 0.1 – 100 Å, one of the options to be used in such a technique. As the refractive index in this X-ray range is almost identical for all materials, there exist no material, i.e. lens, that can focus X-rays as glass can do with visible light for microscopy. Instead, diffraction of X-rays on periodic objects such as 3-dimensional crystals of biomolecules, is used. Therefore, for structure determination by X-ray diffraction analysis one needs to grow high quality crystals of macromolecules. Details of procedures for crystal formation and growth are described below.

1.4.1. Protein crystallization

Obtaining crystals suitable for X-ray diffraction analysis is still the least understood step in the determination of protein structures by biocrystallography methods because the technique relies a lot on a trial-and-error approach. However, there are several principles that form a basis of all crystallization techniques.

First of all, properties of the protein itself are critical for the success of crystallization. Surface amino-acid residues that can participate in crystal contacts; disordered regions in protein molecule (flexible loops) can perturb or prevent the formation of stable crystal contacts; cofactors and post-translational modifications (glycosylation, etc.) either help or hinder crystal formation (67, 68).

High concentrations of protein are needed to increase the probability of interaction between molecules and to overcome the surface tension energy barrier in order to form crystal nuclei. Supersaturation of protein solution is

achieved by increasing the effective protein concentration. For this purpose, precipitant (for example, salt or polyethylene glycol) is added to the protein solution, which affects the packing of water molecules in the protein hydration shell.

Crystals contacts between protein molecules are formed by electrostatic forces, van der Waals and hydrophobic interactions and hydrogen bonding. To enhance the effectiveness of interactions between protein molecules, repulsive forces need to be diminished and attractive forces increased.

Thus, external parameters that affect crystallization are: (1) concentration of protein and precipitant; (2) type of precipitant; (3) pH, which affects charges of surface amino-acid residues and therefore electrostatic forces between protein molecules; (4) temperature, that influences kinetics of crystal growth and strength of hydrophobic interactions (69).

If the protein and/or precipitant concentration is too high, protein molecules will aggregate and form amorphous precipitate. At even higher concentrations phase separation of protein and precipitant solutions occurs. If a protein solution is not saturated, no precipitation or crystallization will occur and the crystallization drop will remain clear. Solubility of a protein in a precipitant solution is illustrated by the phase diagram (Fig. 1.1).

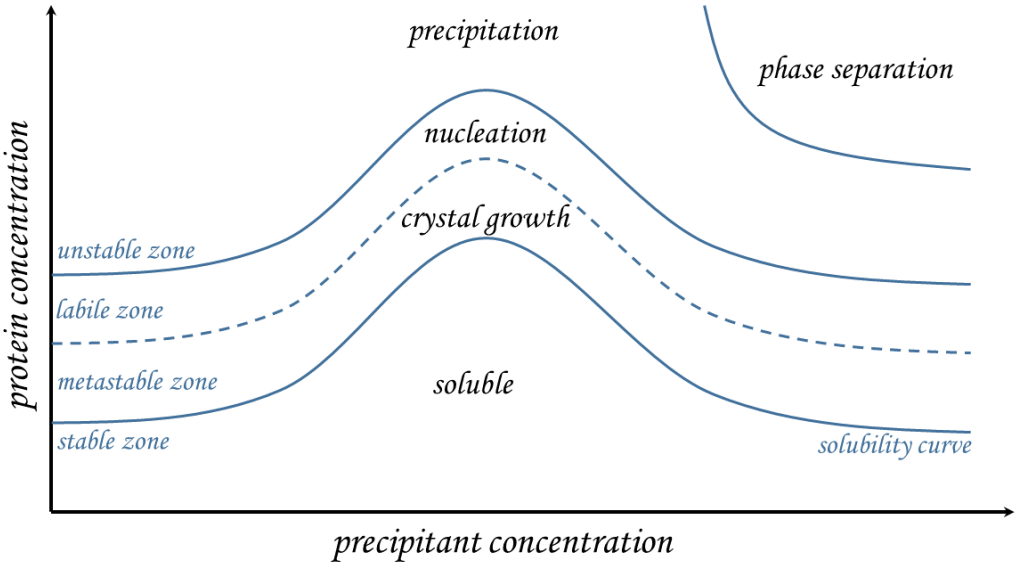

Fig. 1.1. The phase diagram. Crystallizing agent (precipitant) may help to solubilize the protein at low concentrations (salting-in effect), while at higher concentrations it induces decomposition of the solution, namely crystallization or precipitation of the protein as well as phase separation (67).

Various crystallization techniques are nowadays used to achieve supersaturation, including (i) vapor-diffusion techniques, (ii) microbatch under oil, and (iii) counter-diffusion in capillaries. The principle of vapor diffusion methods is to place a drop of protein and precipitant mixture on a cover slide over a reservoir containing precipitant (hanging drop) or on a pedestal over the reservoir (sitting drop) and seal the system to prevent contact with the environment (Fig. 1.2*a*,*b*). Water will evaporate from the drop due to a lower concentration of the crystallizing agent in comparison to the reservoir. With the microbatch under oil technique, a drop of protein and precipitant mixture is pipetted under the layer of mineral oil that either allows evaporation of water (silicon oil or silicon-paraffin mixture) or not (paraffin) (Fig. 1.2*c*). With the counter-diffusion method, protein and precipitant solutions are for example pipetted into different ends of a thin glass capillary such that they can freely diffuse into each other creating a gradient of concentrations. A layer of agarose gel can be placed between protein and precipitant to slow down the diffusion process (67, 70). Supersaturation of the protein, necessary for nuclei formation, can be achieved at some point during diffusion, concentration or to evaporation.

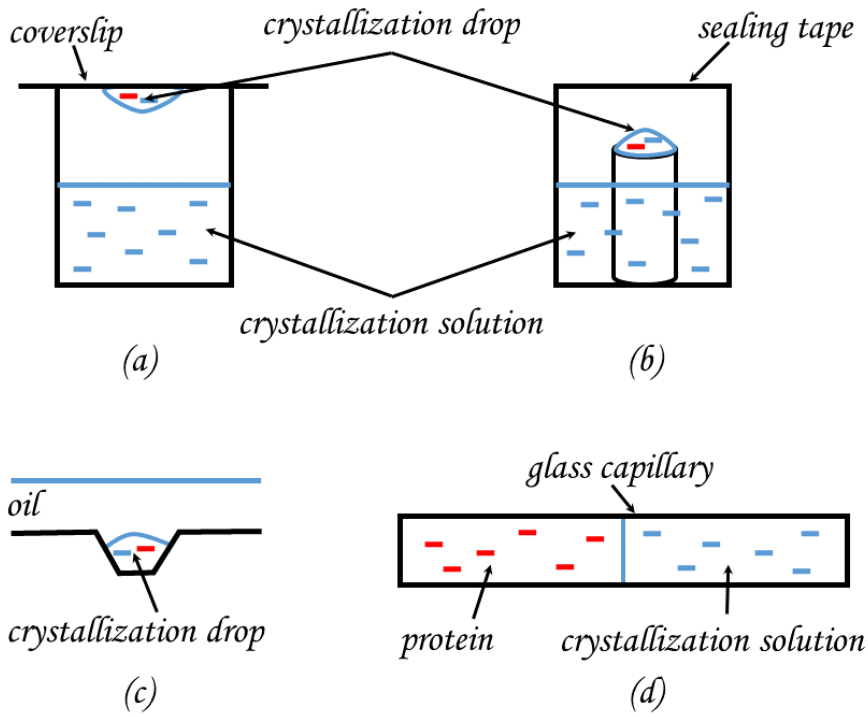

Fig. 1.2. Crystallization techniques: *a*) hanging- and *b*) sitting-drop vapor diffusion; *c*) microbatch under oil; *d*) counter-diffusion in capillaries.

Currently, exact/successful crystallization conditions for a specific protein cannot be predicted. Therefore, crystallization starts with screening various combinations of chemicals. After first successful crystallization conditions are obtained, they often require optimization to enhance the crystal diffraction quality. Optimization can help to stabilize protein molecules, form additional crystal contacts, determine the optimal rate of crystal growth, introduce crystallization centers to aid nucleation. It includes the systematical alteration of protein and precipitant concentrations, pH, temperature and protein-to-precipitant ratio in the crystallization drop. Further optimization steps can include additive screening, micro- and macroseeding of crystals, trying a different crystallization technique, crystallization in low melting point agarose gel, etc. (70, 71).

Properties and symmetry of macromolecular crystals are described in the next section.

1.4.2. Protein crystals properties and symmetry

Protein crystals are periodic arrangements of protein molecules in three-dimensional space forming a crystal lattice (fig. 1.3). Intermolecular contacts between amino acid residues of different protein molecules, are weak, sparse and anisotropically distributed over the crystal volume, and protein molecules themselves are flexible and irregular. Therefore, protein crystals are usually very soft and crush easily, are temperature and pH sensitive, decay if allowed to dehydrate, and undergo extensive damage during prolonged exposure to radiation.

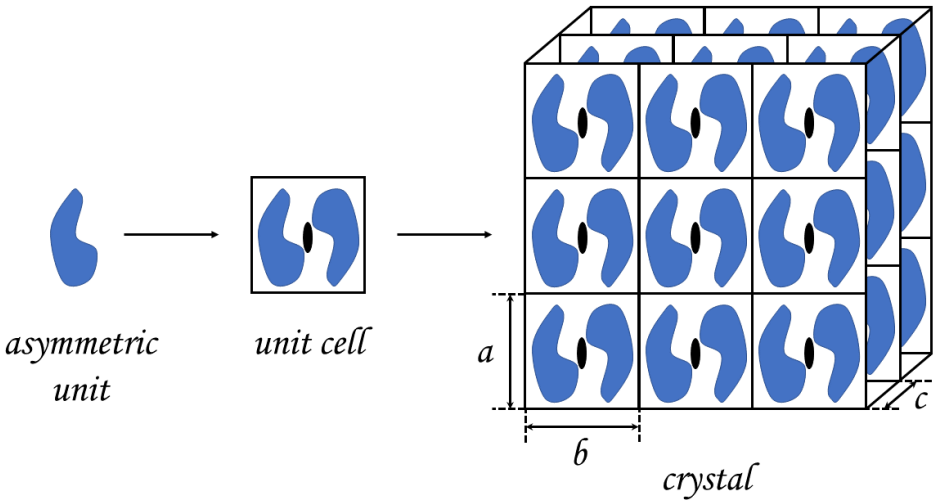

Fig. 1.3. Arrangement of an asymmetric unit into a unit cell by applying for exampletwo-fold crystallographic axis (shown as black ellipse) and subsequent translation about three dimensions in order to form a crystal.

There are 65 different ways in which asymmetric, chiral protein molecules can be arranged into a three-dimensional periodic crystal. These 65 types of arrangement are called space groups (72). A crystal lattice divides crystal space into translationally periodic units, called unit lattice. Unit lattice combined with molecular motif (i.e. one or more biological macromolecules) is called unit cell, therefore, a protein crystal is a finite periodic assembly of unit cells. Each identical unit cell will contain the same number of identically arranged protein molecules and is characterized by axes *a*, *b* and *c* and angles between them α (between axes *b* and *c*), β (axes *a* and *c*), and γ (axes *a* and *b*). The protein

molecules inside the unit cell in turn can be related by symmetry operations, thus, a unit cell may be packed with multiple symmetry equivalent copies of a molecule. The part of the unit cell that contains all necessary information to generate the complete unit cell by applying the symmetry operators is called the asymmetric unit. Allowed symmetry operations for protein crystals are 2-, 3-, 4- and 6-fold rotation and screw axes. Mirror operation, inversion or any combination of symmetry operations including a mirror plane or inversion are not allowed for asymmetric, chiral protein molecules, as these change the handedness of the macromolecule. If an asymmetric unit contains more than one protein molecule, they are related by non-crystallographic symmetry. Non-crystallographic operations are not limited to crystallographic operations and can contain, for example, 5-fold rotation axes, as pentameric molecules assemblies are quite common (67).

1.4.3. Scattering of X-rays on atoms

X-rays are electromagnetic waves that interact with the electrons of an atom, as they are polarizable enough to interact with changing electromagnetic field of such high frequency. The magnetic component impact is much lower than that of the electric field component and is usually neglected in the calculations.

There are three mechanisms of X-ray interaction with electrons: elastic (Rayleigh) scattering; inelastic (Compton) scattering and absorption of X-rays by the electrons of an atom. During elastic scattering X-ray photons do not lose energy through interaction with electrons (i.e. frequency remains the same) but change propagation direction. Summation of such scattered waves results in a diffraction pattern that is used for structure determination. Compton scattering contributes to radiation damage of the sample and increases background noise of the diffraction pattern, as an incoming X-ray photon deposits some amount of energy inside the crystal and is deflected in a random direction with lower frequency. If the energy of an incoming photon equals the energy of a bound electron in the atom, it can be absorbed by the electron creating a vacancy in the electron shell. Vacancy is then filled by another electron that loses energy in form of an X-ray photon. Absorption of X-rays is also called anomalous scattering and is used in experimental phasing techniques (67).

The condition for constructive interference of scattered waves is easy to

derive if one considers the waves scattered in the same direction to be reflected by a parallel set of (imaginary) planes (Fig. 1.4). A signal will be read by the detector if the waves arrive to it in the same phase, i.e. the path difference between the waves is equal to an integer number of wavelengths.

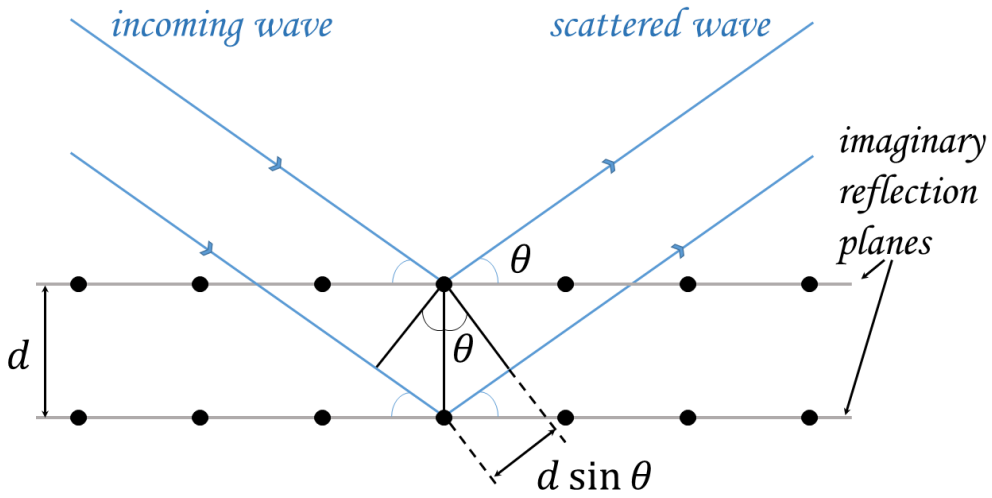

Fig. 1.4. Schematic representation of the incoming X-ray photons scattering on electrons of atoms arranged in a crystal.

The condition for constructive interference is called Bragg's law:

$$n\lambda = 2d \sin\theta \qquad (1.1)$$

where λ is wavelength of the incoming X-ray, n is an integer, d is the distance between planes, θ is the angle between incoming (scattered) wave and plane, and $2d \sin\theta$ is the path difference between waves (67, 69).

1.4.4. The reciprocal lattice and X-ray data collection

Both reciprocal lattice and Ewald sphere (73) are formal constructs used to visualize the concepts of X-ray data collection (Fig. 1.5).

Sets of equidistant and parallel lattice planes (as the one presented in Fig. 1.4) in the real space are described by Miller indices *h*, *k* and *l*, that are integers indicating the number of intersections between set of planes and unit cell axes. Each set of real lattice planes *hkl* corresponds to a reciprocal lattice point with reciprocal lattice vector $\boldsymbol{d}^*_{hkl}$ perpendicular to this set of real lattice planes. The

magnitude of the reciprocal lattice vector is reciprocal to the distance between real lattice planes d_{hkl} (fig. 1.4):

$$d^*_{hkl} = 1/d_{hkl} \qquad (1.2)$$

The Ewald construction is a graphical representation of Bragg's law and consists of a sphere with radius $1/\lambda$ and a reciprocal lattice, as shown in Fig. 1.5. Whenever a reciprocal lattice point touches the Ewald sphere, Bragg's law is fulfilled and a reflection (result of constructive interference) is observed by the detector. To collect more reflections, the crystal is rotated along one or more axes thereby rotating the reciprocal lattice and moving more reciprocal lattice points through the Ewald sphere surface.

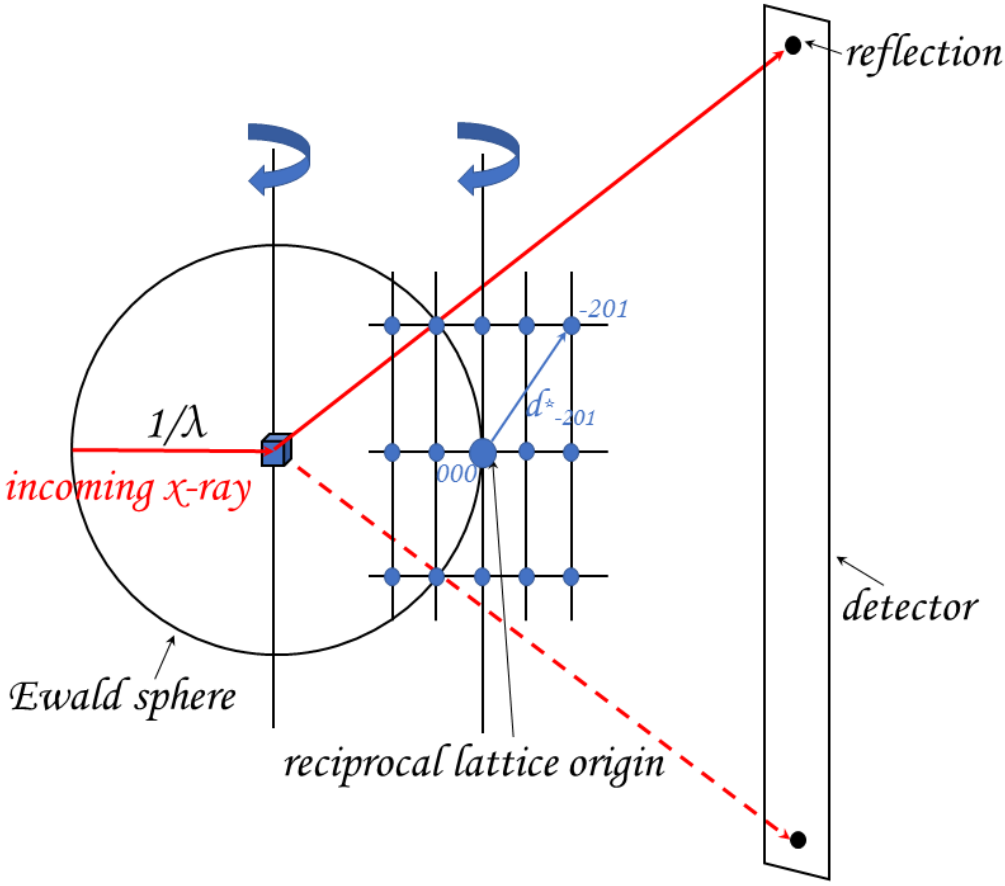

Fig. 1.5. Ewald construction (73).

An important feature of the reciprocal lattice is its centrosymmetry, meaning that reflections hkl and $\overline{hkl}$ have equal intensity (Friedel's law, 74).

1.4.5. Data processing, structure determination and refinement.

Total scattered wave from a crystal in the exact direction (described by Miller indices of a reciprocal lattice point on Ewald sphere) is called structure factor $\boldsymbol{F}(hkl)$ and can be calculated as a Fourier transform of electron density $\rho(xyz)$:

$$\boldsymbol{F}(hkl) = \int_{crystal} \rho(xyz) \exp(2\pi i(hx + ky + lz)) d(xyz) \quad (1.3)$$

where $\rho(xyz)$ is the electron density in a point with coordinates xyz; h, k and l are Miller indices.

The intensities of the reflections on the diffraction pattern are proportional to the amplitude of structure factors $|\boldsymbol{F}(hkl)|$. Therefore, the first steps of data processing, once data collection was finished, are to assign Miller indices to all reflections on all diffraction patterns and integrate partial reflections, and to calculate data collection statistics in order to evaluate the quality of the data.

Electron density can be reconstructed from the structure factors by reverse Fourier transform:

$$\rho(xyz) = \frac{1}{V} \sum_{hkl} |\boldsymbol{F}_{hkl}| \exp(i\varphi) \exp(-2\pi i(hx + ky + lz) \quad (1.4)$$

where $\boldsymbol{F}(hkl) = |\boldsymbol{F}_{hkl}| \exp(i\varphi)$, $|\boldsymbol{F}_{hkl}|$ is the amplitude of structure factor, φ is its phase, and V is the volume of a crystal (67).

To reconstruct electron density not only amplitude of the structure factor is needed but also phase, which cannot be obtained from the diffraction pattern. This is referred to as the phase problem in crystallography. There are several ways to resolve the phase problem such as direct methods, isomorphous replacement, anomalous scattering and molecular replacement (75). In direct methods, the phases of some reflections are known, or can be given a variety of starting values, then the phases of other reflections can be deduced afterwards.

These methods require very high resolution data (<1.2 Å) and calculations are increasingly time-consuming with and increasing number of atoms in the asymmetric unit. Molecular replacement is used when a structurally similar search model to the target protein is available (usually requires sequence identity >25%). The idea of the method is to search for the proper orientation and location of the search model within the unit cell of the unknown target crystal structure and derive phases from the rotated and translated model structure. Isomorphous replacement uses differences in the reflections intensities of a native crystal and crystal soaked with a heavy atom (both crystals must display the same space group and unit cell dimensions) in order to determine the positions of the heavy atoms. Native protein phases are estimated using obtained phases and amplitudes of heavy atoms structure factors. Anomalous scattering leads to a breakdown of Friedel's law, resulting in anomalous differences that can then be used to locate the anomalous scatterers and use their phases to calculate native structure phases (67, 75).

Once a starting model is obtained by any of these phasing techniques, the model is refined further to comply with the electron density maps and validated using known stereochemical restraints.

2. MATERIALS AND METHODS

2.1. Crystallization

The initial screening for crystallization conditions for wild-type glyceraldehyde dehydrogenase from *Thermoplasma acidophilum* (*Ta*AlDHwt) and its variants *Ta*AlDH F34M+S405N and *Ta*AlDH F34M+Y399C+S405N, and for haloalkane dehalogenase LinB from Sphingobium japonicum variants LinB73 and LinB86 was carried out using a Gryphon crystallization robot (Art Robbins Instruments, USA) by the sitting-drop vapour-diffusion method in MRC 2-well crystallization plates (Hampton Research, USA). Protein solution was mixed with reservoir solution in 1:1 and 2:1 ratios and equilibrated against reservoir solution at 277 K and/or at 295 K. Various commercial screens from Hampton Research (USA), Molecular Dimensions (UK) and Qiagen (The Netherlands) were applied for the initial screening.

The first stage of the optimization of crystallization conditions included variation of pH and protein and precipitant concentrations and ratios. Additive Screen (Hampton Research, USA) and/or microseeding procedure (70) were used if crystals required further optimization to obtain reasonable diffraction quality. Optimization experiments were carried out by the sitting-drop vapour-diffusion technique in 24-well CombiClover crystallization plates (Rigaku Reagents, USA) and Cryschem Plates (Hampton Research, USA) at 277 and 295 K.

For the preparation of seed stocks, crystals of the protein were transferred into a drop of reservoir solution with a nylon loop (Hampton Research, USA) and crushed into microseeds using a Seed Bead (Hampton Research, USA), followed by serial dilutions of 1:10 to 1:100 000. 0.5-1 µl of seed stock were then added to 3-6 µl drop of protein and precipitant mixture in different ratios.

The identity of crystallized protein was checked by Coomassie Blue staining of a 12% SDS–PAGE gel using ColorBurst Electrophoresis Marker MW 8–220 kDa (Sigma–Aldrich, USA).

The solutions for optimization were prepared using chemicals from Sigma-Aldrich (USA).

2.2. Soaking with ligands

Prior to adding the substrate for haloalkane dehalogenase LinB variants,

1,2-dibromoethane, the crystals were stabilized by cross-linking procedure. Cross-linking was performed in CombiClover crystallization plates (Rigaku Reagents) at room temperature using sitting drop vapor diffusion technique with microbriges (Hampton Research) to create a separate reservoir for the cross-linking agent (glutaraldehyde). 1-2 µl drop of 25% glutaraldehyde was placed in the well of the microbridge positioned in the reservoir of crystallization plate (76) and the system was sealed with the sealing tape. The reaction proceeded for 10-45 minutes and at the end of the period microbridge was removed from the reservoir and crystals were transferred to a fresh drop of crystallization cocktail.

Substrate soaking experiments were performed both at 277 and 295 K. 20 µl of 1,2-dibromoethane was added to reservoir of CombiClover plate and the system was sealed with the sealing tape for the period from 5 minutes to 4 hours. At the end of the period crystals were fished out from the crystallization drop and flash-cooled in liquid nitrogen for X-ray data collection.

2.3. Data collection

Obtained crystals were tested either at the home X-ray source, Venture D8 (Bruker, USA) system equipped with Photon II CPAD detector or directly at the synchrotron. Diffraction data collections were performed at the BL14.1 beamline operated by the Joint Berlin MX Laboratory at the BESSY II electron-storage ring in Berlin-Adlershof, Germany (77) equipped with a PILATUS 6M detector (Dectris, Switzerland) at 100 K.

Crystals for data collection were mounted in a LithoLoops (Molecular Dimensions, UK), nylon cryoloops (Hampton Research, USA) or MicroLoops (MiTeGen, USA). For testing crystals at room temperature MicroRT system (MiTeGen) was used.

For the data collection at 100 K crystals were cryoprotected before flash-cooling in liquid nitrogen. If the crystallization condition contained sufficient amount of salt or other compound which serves as a cryoprotectant, crystals were fished out for measurements directly from the crystallization drop and flash-cooled in liquid nitrogen without additional cryoprotection. For cryoprotection in case of low concentrations of cryoprotectant in crystallization cocktail one-two microliters of the same compound in higher concentration (40-50% w/v in case of PEGs or 2-3 M in case of salt) were added to crystallization

drop and left for several minutes for soaking. Transferring protein crystals between drops with gradually increased cryoprotectant concentration was used as an alternative way of cryoprotection for very fragile and sensitive crystals. For the conditions not containing cryoprotectant crystals were transferred to the drop of crystallization cocktail mixed with ethylene glycol, glycerol or 2-methyl-2,4-pentanediol for soaking prior to cooling in liquid nitrogen.

Diffraction quality of the crystals was tested by collecting two diffraction images with 1° oscillation angle, second image after 90° rotation compared to the first one. These images were used for estimation of space group, unit cell parameters and data collection strategy calculation using *iMOSFLM* graphical interface for running *MOSFLM* (78). The diffraction data for all crystals were processed using the *XDSAPP* graphical user interface (79) to run *XDS* (80). The solvent content of the crystals was analyzed by calculation of the Matthews coefficient (81) for all data sets using *MATTHEWS_COEF* from the *CCP4* package (82).

2.4. Structure solution and refinement

The structures of all proteins were solved by molecular replacement method using the structure with the highest sequence identity from the PDB. Web-based version of the automated pipeline for molecular replacement *BALBES* (83) or programs *MOLREP* (84) and *PHASER* (85) as a part of *CCP4* were used for different structures. All ligands and water molecules were removed from the coordinates file used as a search model for molecular replacement, and in case of oligomeric structure both monomer and corresponding oligomer were tried out.

REFMAC (86) for automated refinement and *Coot* (87) for manual rebuilding were used for the structure refinement of all proteins at resolution 1.5 Å and lower. At the resolution around 2 Å, non-crystallographic symmetry restraints were used at the early stages of restrained refinement, accompanied by resetting B-factor to the value derived from the Wilson plot and by introducing 0.2-0.3 Å noise into the coordinates before each cycle of automated refinement. B-factors were refined isotropically. At a later stage, TLS (translation-libration-screw) restraints were introduced (88) for several structures. Waters were added at the positions where the level of the difference F_o-F_c map exceeded 3σ and given reasonable distance and geometric constraints

with neighboring amino acids residues.

For resolution 1.5 Å water molecules were refined with isotropic B-factors, atoms in protein molecules and ligands with anisotropic refinement of B-factors. Choice for anisotropic refinement was based on Hamilton R-ratio test (89, 90), and on overall better quality of electron density map after anisotropic refinement in contrast to the map with isotropic refinement of B-factors.

Low-resolution refinement (lower than 3.0 Å) was done using *ProSMART* (91) to generate fragment restraints followed by isotropic B-factor refinement in *REFMAC*. Given the resolution, no water molecules or ligands were added.

High-resolution refinement (1.1 Å and higher) was performed using *SHELXL* (92) with anisotropic refinement of individual B-factors for all atoms in an asymmetric unit. *Coot* was used for the manual validation and refinement.

The model geometry (e.g. bond length, angles, Ramachandran plot, clashes) and agreement between the structure and the experimental data were validated using *Coot*, *PDB_REDO* (93) and wwPDB Validation Server at http://wwpdb-validation.wwpdb.org/validservice/.

2.5. Structure analysis

Interaction surfaces between monomers in either dimer or tetramer were analyzed by means of *PISA Interfaces* (94) from within the *Coot* package. *CAVER Analyst* (95) was used for locating accession tunnels in the enzyme structures, with probe radius 1.0 Å.

3. RESULTS AND DISCUSSION

3.1. Crystallization behaviour of glyceraldehyde dehydrogenase from *Thermoplasma acidophilum*

This chapter is based on Paper I:

Iermak I, Degtjarik O, Steffler F, Sieber V, Kuta Smatanova I (2015) Crystallization behaviour of glyceraldehyde dehydrogenase from Thermoplasma acidophilum. *Acta Cryst F* 71:1475-1480.

ABSTRACT

The glyceraldehyde dehydrogenase from *Thermoplasma acidophilum* (*Ta*AlDH) is a microbial enzyme that catalyzes the oxidation of D-glyceraldehyde to D-glycerate in the artificial enzyme cascade designed for the conversion of glucose to the organic solvents isobutanol and ethanol. Various mutants of *Ta*AlDH were constructed by random approach followed by site-directed and saturation mutagenesis in order to improve enzyme properties essential for its functioning within the cascade. Two enzyme variants, *Ta*AlDH wild type and mutant *Ta*AlDH F34M+S405N were crystallized successfully. Crystals of *Ta*AlDHwt belong to monoclinic $P12_11$ space group with 8 molecules per asymmetric unit and diffracted to the resolution of 1.95 Å. *Ta*AlDH F34M+S405N crystallizes in two different space groups: triclinic *P*1 with 16 molecules per asymmetric unit and monoclinic *C*121 with 4 molecules per asymmetric unit. These crystals diffracted to the resolutions of 2.14 and 2.10 Å for *P*1 and *C*121, respectively.

3.2. Structural features of glyceraldehyde dehydrogenase from *Thermoplasma acidophilum*

This chapter is based on Paper II:

Iermak I, Mesters JR, Steffler F, Sieber V, Kuta Smatanova I (2017) Structural features of glyceraldehyde dehydrogenase from *Thermoplasma acidophilum*. *Manuscript*.

ABSTRACT

Glyceraldehyde dehydrogenase from *Thermoplasma acidophilum* (*Ta*AlDH) catalyzes the oxidation of D-glyceraldehyde to D-glycerate, which is one of the key reactions of the pathway for the production of ethanol and isobutanol. The enzyme was selected for its high substrate specificity and thermostability and was successfully implemented in the cascade. However, further optimization is required to enhance *Ta*AlDH functioning within the cell-free system, including NAD^+ acceptance, product tolerance and overall activity. The cascade is intended to function as completely redox balanced and to use only a single molecular electron shuttle NAD^+ (as the majority of used enzymes are NAD^+-dependent), which is recycled within the cascade.

In this article, we report models of the crystal structures of the wild-type *Ta*AlDH and two variants, that were obtained by a random evolution approach. The experimentally obtained structures will be used for the rational design of the enzyme.

3.3. Engineering a *de novo* transport tunnel.

This chapter is based on Paper III:

Brezovsky J, Babkova P, Degtjarik O, Fortova A, Gora A, Iermak I, Rezacova P, Dvorak P, Kuta Smatanova I, Prokop Z, Chaloupkova R, Damborsky J (2016) Engineering a *de novo* transport tunnel. *ACS Catalysis*, 6(11):7597-7610.

ABSTRACT

Transport of ligands between buried active sites and bulk solvent is a key step in the catalytic cycle of many enzymes. Absence of evolutionary optimized transport tunnels is an important barrier limiting the efficiency of biocata-lysts prepared by computational design. Creating a structurally defined and functional “hole” into the protein represents an engineering challenge. Here we describe the computational design and directed evolution of a de novo transport tun-nel in haloalkane dehalogenase. Mutants with a closed native tunnel and newly opened auxiliary tunnel in a distinct part of the structure showed dramatically modified properties. The attained enzymes showed specificity never observed for native family members including the most proficient haloalkane dehalogenase reported to date. Crystallographic analysis and molecular dynamics simulations confirmed successful introduction of the new tunnel. The results demonstrated the power of enzymes with de novo transport tunnels. We anticipate that this engineering strategy will facilitate creation of a wide range of useful biocatalysts.

3.4. Structural features of haloalkane dehalogenase LinB variants

This chapter is based on Paper IV:

Iermak I, Mesters JR, Chaloupkova R, Damborsky J, Kuta Smatanova I (2017) Structural features of haloalkane dehalogenase LinB variants. *Manuscript*.

ABSTRACT

Haloalkane dehalogenases are bacterial enzymes that convert a wide range of halogenated environmental pollutants to the corresponding alcohol, a halide ion and a proton. These enzymes have the potential for application in biosensing and biodegradation of halogenated compounds in soil and groundwater, as well as other biotechnological applications.

Haloalkane dehalogenase LinB isolated from the soil bacterium *Sphingobium japonicum* UT26 has a broad substrate specificity compared to the other enzymes from the haloalkane dehalogenase family. Different variants of haloalkane dehalogenase LinB were constructed with a goal to study the effect of amino-acid substitutions on enzyme function. Amino-acid substitutions in LinB73 (D147C+L177C) cause blocking of the main tunnel in the variant protein by formation of a disulphide bridge. In LinB86 variant W140A+F143L+L177W+I211L the main tunnel is obstructed by a bulky tryptophan, while an alternative pathway is opened between the deeply buried active site and the surrounding solvent. Both structures were solved using X-ray crystallographic techniques. The LinB73 structure, refined to a resolution of 1.15 Å, revealed that disulfide bond is formed only fractionally and is affected by crystal contacts. Successful introduction of a *de-novo* transport tunnel in LinB86 was reported previously and the aim of the current study was to investigate the details of the reaction mechanism. Two post-cleavage reaction snapshots were revealed using 1,2-dibromoethane as a substrate.

4. CONCLUSIONS

After first organisms were employed in industrial applications, the question arose regarding their optimization for more efficient usage. Genetic engineering along with the metabolic engineering has been used as an optimization tool for the cell-based approaches for decades. Development of structural biology techniques opened additional possibilities for the rational design of cell-based biosynthesis as well as for improvement of cell-free pathways. Currently, such techniques as X-ray crystallographic analysis and NMR are widely employed in the construction of biotechnologically effective enzymes and their combinations, as the structural information is valuable for the understanding of enzymes' functions.

This thesis includes two projects. The first part is focused on the structure-functional analysis of glyceraldehyde dehydrogenase from *Thermoplasma acidophilum* (*Ta*AlDH) for employment in cell-free enzyme cascade for biosynthesis of ethanol or isobutanol from glucose. Aldehyde dehydrogenase catalyzes the conversion of glyceraldehyde to glycerate, one of the key reactions within the pathway. The enzyme needs to possess high substrate specificity to avoid side-product production. *Ta*AlDH was selected to be applied in the enzyme cascade due to its high specificity towards glyceraldehyde and optimized by random evolution approach to improve other properties essential for functioning within the cascade (21). For further rational enhancement of the enzyme X-ray diffraction analysis of the crystals of *Ta*AlDH and its constructed variants was carried out.

Wild-type *Ta*AlDH and *Ta*AlDH F34M+S405N and *Ta*AlDH F34M+Y399C+S405N variants displayed an unusual crystallization behaviour; crystals of each of the variants were found in 20-30 different conditions (Iermak et al, 2015). Only several crystallization conditions were selected for optimization based on the next criteria: (i) the already known diffraction quality of the crystals, (ii) the size and shape of the crystals (large single crystals with sharp edges are preferred) and (iii) visually different crystal forms (to check as many different variants of protein-molecule packing inside the crystal as possible). Interestingly, the best resolution of the diffraction was obtained for crystals from quite different conditions for each of *Ta*AlDH variants, although they differ only in few amino acids.

Structurally, wild-type *Ta*AlDH is a homotetramer composed of two homodimers, that are connected *via* β-sheet extension. Active site residues, Glu247 and Cys281, are located inside the protein molecule and are connected to $NADP^+$-binding pocket on the surface by the tunnel. The second end of the tunnel also connects active site with the bulk solvent and, most likely, is used for substrate and product transport between active site and solvent. Amino acids, substituted in *Ta*AlDH F34M+S405N and *Ta*AlDH F34M+Y399C+S405N variants, do not display any contact with the active site or $NADP^+$-binding cavity. Therefore, these amino-acid substitutions have indirect and subtle effect on enzyme's properties.

As the cascade for alcohols biosynthesis is intended to use and recycle single molecular electron shuttle NAD^+, *Ta*AlDH should be optimized to prefer NAD^+ as a cofactor. Analysis of $NADP^+$-binding pocket of wild-type *Ta*AlDH helped to uncover amino acid residues, potentially responsible for the of interaction with $NADP^+$. Site-directed mutagenesis of the identified residues is planned in order to check our idea experimentally.

The second part of thesis describes structure-functional analysis and structure-based rational design of haloalkane dehalogenase LinB variants. Haloalkane dehalogenases are bacterial enzymes that catalyse cleavage of halogen-carbon bond in a wide range of halogenated environmental pollutants. Haloalkane dehalogenase LinB, isolated from a soil bacterium *Sphingobium japonicum* UT26, is a promising target for biotechnological degradation of halogenated compounds due to its broad substrate specificity (60). Several variants of LinB were constructed in order to study the effects of the mutations on enzyme's properties.

The active site of LinB is situated between cap and core domains of the enzyme, and is connected to the bulk solvent by several tunnels. Tunnels play an important role in the activity and catalytic efficiency of LinB and their alterations cause major changes in enzyme's kinetic parameters (Brezovsky et al, 2016). Blocking of the main access tunnel by the introduction of bulky amino-acid residues resulted in the dramatic decrease of activity, while opening a *de novo* transport tunnel enhanced catalytic efficiency. Although we cannot accurately predict all the effects of amino-acid substitutions in access tunnels, the proposed strategy for opening transport tunnels could be useful for protein engineering of biocatalysts.

The details of the reaction mechanism were investigated for LinB variant with the highest catalytic efficiency due to *de novo* introduced tunnel, LinB86 (LinB-Open^{W}). Two post-cleavage snapshots were revealed using 1,2-dibromoethane as a substrate, illustrating the starting positions of the products for the transport through the tunnel and release into the bulk solvent. Further studying of reaction stages for different LinB mutants will complete the understanding of enzyme functioning and the effects of the tunnels engineering on catalytic properties of the enzyme.

5. REFERENCES

1. Benner SA, Sismour AM (2005) Synthetic biology. Nat Rev Genetics 6(7):533–543.

2. Ylitervo P, Franzén CJ, Taherzadeh MJ (2011) Ethanol production at elevated temperatures using encapsulation of yeast. J Biotechnol 156(1):22–29.

3. Atsumi S, Wu T-Y, Machado IMP, Huang W-C, Chen PY, Pellegrini M, James CL (2010) Evolution, genomic analysis, and reconstruction of isobutanol tolerance in *Escherichia coli*. Mol Syst Biol 6(1):449.

4. Lee SY, Park JH, Jang SH, Nielsen LK, Kim J, Jung KS (2008) Fermentative butanol production by *Clostridia*. Biotechnol Bioeng 101(2):209–228.

5. Zhang YHP, Evans BR, Mielenz JR, Hopkins RC, Adams MWW (2007) High-yield hydrogen production from starch and water by a synthetic enzymatic pathway. PLoSONE, 2(5):e456.

6. Chang MCY, Eachus RA, Trieu W, Ro D-K, Keasling JD (2007) Engineering *Escherichia coli* for production of functionalized terpenoids using plant P450s. Nat Chem Biol 3(5):274-277.

7. Lee KH, Park JH, Kim TY, Kim HU, Lee SY (2007) Systems metabolic engineering of *Escherichia coli* for L-threonine production. Mol Syst Biol 3(1):149.

8. Roessner CA, Scott AI (1996) Genetically engineered synthesis of natural products: from alkaloids to corrins. Ann Rev Microbiol 50(1):467–490.

9. Jung YK, Kim TY, Park SJ, Lee SY (2010) Metabolic engineering of *Escherichia coli* for the production of polylactic acid and its copolymers. Biotechnol Bioeng 105(1):161-171.

10. Savage DF, Way J, Silver PA (2008) Defossiling fuel: how synthetic biology can transform biofuel production. ACS Chem Biol 3(1):13-16.

11. Rupp S (2013) Next-generation bioproduction systems: cell-free conversion concepts for industrial biotechnology. Eng Life Sci 13(1):19–25.

12. Jia K, Zhang Y, Li Y (2010) Systematic engineering of microorganisms to improve alcohol tolerance. Eng Life Sci 10(5):422–429.

13. Guterl J-K, Sieber V (2013) Biosynthesis “debugged”: novel bioproduction strategies. Eng Life Sci 13(1):4-18.

14. Hodgman CE, Jewett MC (2012) Cell-free synthetic biology: thinking

outside the cell. Metab Eng 14(3):261–269.

15. Khattak WA, Ullah MW, Ul-Islam M, Khan S, Kim M, Kim Y and Park JK (2014) Developmental strategies and regulation of cell-free enzyme system for ethanol production: a molecular prospective. Appl Microbiol Biotechnol 98(23):9561-9578.

16. Zhang Y-HP (2010) Production of biocommodities and bioelectricity by cell-free synthetic enzymatic pathway biotransformations: challenges and opportunities. Biotechnol Bioeng 105(4):663–677.

17. Shimizu Y, Inoue A, Tomari Y, Suzuki T, Yokogawa T, Nishikawa K, Ueda T (2001) Cell-free translation reconstituted with purified components. Nat Biotechnol 19(8):751–755.

18. Buchner E (1897) Alkoholische gahrung ohne hefezellen. Ber Chem Ges 30:117–124.

19. Ahmed H, Ettema TJ, Tjaden B, Geerling AC, van der Oost J, Siebers B (2005) The semi-phosphorylative Entner–Doudoroff pathway in hyperthermophilic archaea: a re-evaluation. Biochem J 390(2):529-540.

20. Guterl J-K, Garbe D, Carsten J, Steffler F, Sommer B, Reiße S, Philipp A, Haack M, Ruhmann B, Koltermann A, Kettling U, Bruck T, Sieber V (2012) Cell-free metabolic engineering: production of chemicals by minimized reaction cascades. ChemSusChem 5(11):2165–2172.

21. Steffler F, Guterl J-K, Sieber V (2013) Improvement of thermostable aldehyde dehydrogenase by directed evolution for application in Synthetic Cascade Biomanufacturing. Enzyme Microb Technol 53(5):307– 314.

22. Jung JH, Lee SB (2006) Identification and characterization of *Thermoplasma acidophilum* glyceraldehyde dehydrogenase: a new class of $NADP^+$-specific aldehyde dehydrogenase. Biochem J 397(1):131-138.

23. Steffler F, Sieber V (2013) Refolding of a thermostable glyceraldehyde dehydrogenase for application in synthetic cascade biomanufacturing. PLoSONE 8(7):e70592.

24. Falta RW (2004) The potential for ground water contamination by the gasoline lead scavengers ethylene dibromide and 1,2-dichloroethane. Ground Water Monit Rem 24(3):76–87.

25. Aronson D, Howard PH (2008) The environmental behavior of ethylene dibromide and 1,2-dichloroethane in surface water, soil, and groundwater. API Publication 4774.

26. Li YF, Bidleman TF, Barrie LA, McConnell LL (1998) Global hexachlorocyclohexane use trends and their impact on the arctic atmospheric environment. Geophys Res Lett 25(1):39-41.

27. Lallas P (2001) The Stockholm convention on persistent organic pollutants. AJIL 95(3):692-708.

28. Falta RW, Bulsara N, Henderson JK, Mayer RA (2005) Leaded-gasoline additives still contaminate groundwater. Environ Sci Technol 39:378A-384A.

29. Steinberg SM, Pignatello JJ, Shawhney BL (1987) Persistence of 1,2-dibromoethane in soils: entrapment in intraparticle micropores. Environ Sci Technol 21(12), 1201–1208.

30. Wilson JT, Banks K, Earle RC, He Y, Kuder T, Adair C (2008) Natural attenuation of the lead scavengers 1,2-dibromoethane (EDB) and 1,2-dichloroethane (1,2-DCA) at motor fuel release sites and implications for risk management. EPA Washington, D.C. EPA/600/R-08/107.

31. Schwartzenbach RP, Giger W, Schaffner C, Wanner O (1985) Groundwater contamination by volatile halogenated alkanes: abiotic formation of volatile sulfur compounds under anaerobic conditions. Environ Sci Technol 19(4):322–327.

32. Belay N, Daniels L (1987) Production of ethane, ethylene, and acetylene from halogenated hydrocarbons by methanogenic bacteria. Appl Environ Microbiol 53(7):1604–1610.

33. Yu R, Peethambaram HS, Falta RW, Verce MF, Henderson JK, Bagwell CE, Brigmon RL, Freedman DL (2013) Kinetics of 1,2-dichloroethane and 1,2-dibromoethane biodegradation in anaerobic enrichment cultures. Appl Environ Microbiol 79(4):1359–1367.

34. Swindoll CM, Aelion CM, Dobbins DC, Jiang O, Long SC, Pfaender FK (1988) Aerobic biodegradation of natural and xenobiotic organic compounds by subsurface microbial communities. Environ Toxicol Chem 7(4):291–299.

35. Poelarends GJ, van Hylckama Vlieg JE, Marchesi JR, Dos Santos LM, Janssen DB (1999) Degradation of 1, 2-Dibromoethane by *Mycobacterium sp.* Strain GP1. J Bacteriol 181(7):2050-2058.

36. Hartzell KE, Burton CD, Leeson A, Biodegradation of ethylene dibromide through cometabolic mechanisms. In: Leeson A, Johnson PC,

Hinchee RE, Semprini L, Magar VS, Eds. (2001) In situ aeration and aerobic remediation. Battelle Press, Columbus, OH, pp 193–200.

37. Vannelli T, Logan M, Arciero DM, Hooper AB (1990) Degradation of halogenated aliphatic compounds by the ammonia-oxidizing bacterium *Nitrosomonas europaea*. Appl Environ Microbiol 56(4):1169–1171.

38. Hatzinger PB, Streger SH, Begley JF (2015) Enhancing aerobic biodegradation of 1, 2-dibromoethane in groundwater using ethane or propane and inorganic nutrients. J Contam Hydrol 172:61-70.

39. Baek K, Wang M, McKeever R, Rieber K, Park C, Nüsslein K (2014) Biodegradation of low concentrations of 1, 2-dibromoethane in groundwater is enhanced by phenol. Appl Microbiol Biotechnol 98(3):1329-1338.

40. Janssen DB, Dinkla IJT, Poelarends GJ, Terpstra P (2005) Bacterial degradation of xenobiotic compounds: evolution and distribution of novel enzyme activities. Environ Microbiol 7(12):1868–1882.

41. Stucki G, Thueer M (1995) Experiences of a large-scale application of 1,2-dichloroethane degrading microorganisms for groundwater treatment. Environ Sci Technol 29(9):2339–2345.

42. Sato Y, Monincová M, Chaloupková R, Prokop Z, Ohtsubo Y, Minamisawa K, Tsuda M, Damborský J, Nagata Y (2005) Two rhizobial strains, *Mesorhizobium loti* MAFF303099 and *Bradyrhizobium japonicum* USDA110, encode haloalkane dehalogenases with novel structures and substrate specificities. Appl Environ Microbiol 71(8):4372-4379.

43. Campbell DW, Muller C, Reardon KF (2006) Development of a fiber optic enzymatic biosensor for 1,2-dichloroethane. Biotechnol Lett 28(12):883–887.

44. Bidmanova S, Chaloupkova R, Damborsky J, Prokop Z (2010) Development of an enzymatic fiber-optic biosensor for detection of halogenated hydrocarbons. Anal Bioanal Chem 398(5):1891-1898.

45. Prokop Z, Sato Y, Brezovsky J, Mozga T, Chaloupkova R, Koudelakova T, Jerabek P, Stepankova V, Natsume R, van Leeuwen J, Janssen D, Florian J, Nagata Y, Senda T, Damborsky J (2010) Enantioselectivity of haloalkane dehalogenases and its modulation by surface loop engineering. Angew Chem 122(35):6247-51.

46. Los GV, Encell LP, McDougall MG, Hartzell DD, Karassina N, Zimprich C, Wood MG, Learish R, Ohana RF, Urh M, Simpson D, Mendez J,

Zimmerman K, Otto P, Vidugiris G, Zhu J, Darzins A, Klaubert DH, Bulleit RF, Wood KV (2008) HaloTag: A novel protein labelling technology for cell imaging and protein analysis. ACS Chem Biol 3(6):373-382.

47. Bohác M, Nagata Y, Prokop Z, Prokop M, Monincová M, Tsuda M, Koca J, Damborský J (2002). Halide-stabilizing residues of haloalkane dehalogenases studied by quantum mechanic calculations and site-directed mutagenesis. Biochemistry 41(48):14272-14280.

48. Damborský J, Kutý M, Němec M, & Koca J (1997) A molecular modeling study of the catalytic mechanism of haloalkane dehalogenase: 1. quantum chemical study of the first reaction step. J Chem Inform Comput Sci 37(3):562-568.

49. Franken SM, Rozeboom HJ, Kalk KH, Dijkstra BW (1991) Crystal structure of haloalkane dehalogenase: an enzyme to detoxify halogenated alkanes. EMBO J 10(6):1297.

50. Marek J, Vévodová J, Smatanová IK, Nagata Y, Svensson LA, Newman J, Takagi M, Damborský J (2000) Crystal structure of the haloalkane dehalogenase from *Sphingomonas paucimobilis* UT26. Biochemistry 39(46):14082-14086.

51. Mazumdar PA, Hulecki JC, Cherney MM, Garen CR, & James MN (2008) X-ray crystal structure of *Mycobacterium tuberculosis* haloalkane dehalogenase Rv2579. BBA - Proteins and Proteomics 1784(2):351-362.

52. Newman J, Peat TS, Richard R, Kan L, Swanson PE, Affholter JA, Holmes IH, Schindler JF, Unkefer CJ, Terwilliger TC (1999) Haloalkane dehalogenases: structure of a *Rhodococcus* enzyme. Biochemistry 38(49):16105-16114.

53. Ollis DL, Cheah E, Cygler M, Dijkstra B, Frolow F, Franken SM, Harel M, Remington SJ, Silman I, Schrag J, Sussman JL (1992) The α/β hydrolase fold. Protein Eng 5(3):197–211.

54. Janssen DB (2004) Evolving haloalkane dehalogenases. Curr Opin Chem Biol 8(2):150-159.

55. Verschueren KH, Seljee F, Rozeboom HJ, Kalk KH, Dijkstra BW (1993) Crystallographic analysis of the catalytic mechanism of haloalkane dehalogenase. Nature 363(6431):693.

56. Koudelakova T, Chovancova E, Brezovsky J, Monincova M, Fortova A, Jarkovsky J, Damborsky J (2011) Substrate specificity of haloalkane

dehalogenases. Biochem J, 435(2):345–354.

57. Chaloupková R, Sýkorová J, Prokop Z, Jesenská A, Monincová M, Pavlová M, Tsuda M, Nagata Y, Damborský J (2003) Modification of activity and specificity of haloalkane dehalogenase from *Sphingomonas paucimobilis* UT26 by engineering of its entrance tunnel. J Biol Chem 278(52):52622-52628.

58. Liskova V, Bednar D, Prudnikova T, Rezacova P, Koudelakova T, Sebestova E, Kuta Smatanova I, Brezovsky J, Chaloupkova R, Damborsky J (2015). Balancing the stability-activity trade-off by fine-tuning dehalogenase access tunnels. ChemCatChem, 7(4):648-659.

59. Bidmanova S, Damborsky J, Prokop Z (2013) Immobilization of haloalkane dehalogenase LinB from *Sphingobium japonicum* UT26 for biotechnological applications. J Biocatal Biotransformation 2:1.

60. Nagata Y, Miyauchi K, Damborsky J, Manova K, Ansorgova A, Takagi M (1997) Purification and characterization of a haloalkane dehalogenase of a new substrate class from a g-hexachlorocyclohexane-degrading bacterium, S*phingomonas paucimobilis* UT26. Appl Environ Microbiol 63(9):3707–3710.

61. Kmunícek J, Hynková K, Jedlicka T, Nagata Y, Negri A, Gago F, Wade RC, Damborský J (2005) Quantitative analysis of substrate specificity of haloalkane dehalogenase LinB from *Sphingomonas paucimobilis* UT26. Biochemistry 44(9):3390-401.

62. Negri A, Marco E, Damborsky J, Gago F (2007) Stepwise dissection and visualization of the catalytic mechanism of haloalkane dehalogenase LinB using molecular dynamics simulations and computer graphics. J Mol Graph Model 26(3):643-651.

63. Smatanova I, Nagata Y, Svensson LA, Takagi M, Marek J (1999) Crystallization and preliminary X-ray diffraction analysis of haloalkane dehalogenase LinB. Acta Cryst D 55(6):1231-1233.

64. Degtjarik O, Chaloupkova R, Rezacova P, Kuty M, Damborsky J, Kuta Smatanova I (2013) Differences in crystallization of two LinB variants from *Sphingobium japonicum* UT26. Acta Cryst D 69(3):284–287.

65. Biedermannová L, Prokop Z, Gora A, Chovancová E, Kovács M, Damborský J, Wade RC (2012) A single mutation in a tunnel to the active site changes the mechanism and kinetics of product release in haloalkane dehalogenase LinB. J Biol Chem 287(34):29062-29074.

66. Hladilkova J, Prokop Z, Chaloupkova R, Damborsky J, Jungwirth P

(2013). Release of halide ions from the buried active site of the haloalkane dehalogenase LinB revealed by stopped-flow fluorescence analysis and free energy calculations. J Phys Chem B 117(46):14329-14335.

67. Rupp B (2009) Biomolecular crystallography: principles, practice, and application to structural biology. Garland Science.

68. Mesters JR, Hilgenfeld R (2007) Protein Glycosylation, Sweet to Crystal Growth? Cryst Growth Des, 7(11):2251-2253.

69. Drenth J (1999) Principles of protein X-ray crystallography. Springer, New York.

70. Bergfors TM (1999) Protein Crystallization. International University Line, La Jolla, CA.

71. Biertümpfel C, Basquin J, Suck D, Sauter C (2002) Crystallization of biological macromolecules using agarose gel. Acta Cryst D 58(10):1657-1659.

72. Aroyo MA (2016) International tables for crystallography volume A: Space-group symmetry. Wiley.

73. Ewald PP (1921) Die Berechnung optischer und elektrostatischer Gitterpotentiale. Ann Phys 369(3):253-287.

74. Friedel G (1913) Sur les symétries cristallines que peut révéler la diffraction des rayons Röntgen. CR Acad Sci 157:1533-1536.

75. Taylor G (2003) The phase problem. Acta Cryst D 59(11):1881-1890.

76. Lusty CJ (1999) A gentle vapor-diffusion technique for cross-linking of protein crystals for cryocrystallography. J Appl Crystallogr 32(1):106-112.

77. Mueller U, Darowski N, Fuchs MR, Forster R, Hellmig M, Paithankar KS, Puhringer S, Steffien M, Zocher G, Weiss MS (2012) Facilities for macromolecular crystallography at the Helmholtz-Zentrum Berlin. J Synchrotron Rad 19(3):442-449.

78. Battye TG, Kontogiannis L, Johnson O, Powell HR, Leslie AG (2011) iMOSFLM: a new graphical interface for diffraction-image processing with MOSFLM. Acta Cryst D 67(4):271-281.

79. Krug M, Weiss MS, Heinemann U, Mueller U (2012) XDSAPP: a graphical user interface for the convenient processing of diffraction data using XDS. J Appl Crystallogr 45(3):568-572.

80. Kabsch W (2010) XDS. Acta Cryst D 66(2):125-132.

81. Matthews BW (1968) Solvent content of protein crystals. J Mol Biol 33(2):491–497.

82. Winn MD, Ballard CC, Cowtan KD, Dodson EJ, Emsley P, Evans PR, Keegan RM, Krissinel EB, Leslie AG, McCoy A, McNicholas SJ (2011) Overview of the CCP4 suite and current developments. Acta Cryst D 67(4):235-242.

83. Long F, Vagin AA, Young P, Murshudov GN (2008) BALBES: a molecular-replacement pipeline. Acta Cryst D 64(1):125-132.

84. Vagin A, Teplyakov A (1997) MOLREP: an automated program for molecular replacement J Appl Cryst 30(6):1022-1025.

85. McCoy AJ, Grosse-Kunstleve RW, Adams PD, Winn MD, Storoni LC, Read RJ (2007) Phaser crystallographic software. J Appl Cryst 40(4):658-674.

86. Murshudov GN, Skubák P, Lebedev AA, Pannu NS, Steiner RA, Nicholls RA, Winn MD, Long F, Vagin AA (2011) REFMAC5 for the refinement of macromolecular crystal structures. Acta Cryst D 67(4):355-367.

87. Emsley P, Lohkamp B, Scott WG, Cowtan K (2010) Features and development of Coot. Acta Cryst D 66(4):486-501.

88. Winn MD, Isupov MN, Murshudov GN (2001) Use of TLS parameters to model anisotropic displacements in macromolecular refinement. Acta Cryst D 57(1):122-133.

89. Hamilton WC (1965) Significance tests on the crystallographic R factor. Acta Cryst 18(3):502-510.

90. Merritt EA (2012) To B or not to B: a question of resolution? Acta Cryst D 68(4):468-477.

91. Nicholls RA, Long F, Murshudov GN (2012) Low Resolution Refinement Tools in REFMAC5. Acta Cryst D 68(4):404-417.

92. Sheldrick GM, Schneider TR (1997) [16] SHELXL: High-resolution refinement. Methods Enzymol 277:319-343.

93. Joosten RP, Joosten K, Murshudov GN, Perrakis A (2012) PDB_REDO: constructive validation, more than just looking for errors. Acta Cryst D 68:484-496.

94. Krissinel E, Henrick K (2007) Inference of macromolecular assemblies from crystalline state. J Mol Biol 372(3):774-797.

95. Kozlikova B, Sebestova E, Sustr V, Brezovsky J, Strnad O, Daniel L, Bednar D, Pavelka A, Manak M, Bezdeka M, Benes P (2014) CAVER Analyst 1.0: Graphic tool for interactive visualization and analysis of tunnels and

channels in protein structures. Bioinformatics 30(18):2684-2685.

julia.ermak90@gmail.com

Structural biology approach to biotechnological problems
Ph.D. Thesis Series, 2017, No. 6

Printed in the Czech Republic by Typodesign
Edition of 20 copies

University of South Bohemia in České Budějovice
Faculty of Science
Branišovská 1760
CZ-37005 České Budějovice, Czech Republic

Phone: +420 387 776 201 www.prf.jcu.cz, e-mail: sekret-fpr@prf.jcu.cz